Supplementary Information for

"Continuous Heteroepitaxy of Two-Dimensional Heterostructures Based on Layered Chalcogenides"

Yu Kobayashi[1], *Shoji Yoshida*[2], *Mina Maruyama*[2], *Hiroyuki Mogi*[2], *Kota Murase*[2], *Yutaka Maniwa*[1], *Osamu Takeuchi*[2], *Susumu Okada*[2], *Hidemi Shigekawa*[2], *Yasumitsu Miyata*[1,*]

[1] Department of Physics, Tokyo Metropolitan University, Hachioji, Tokyo 192-0397, Japan
[2] Faculty of Pure and Applied Sciences, University of Tsukuba, Tsukuba 305-8573, Japan

Table S1. Growth parameters for WS_2, WSe_2, MoS_2 and $MoSe_2$ monolayers in the present study.

	Flow rate for bubbling of transition metal precursors	Flow rate for bubbling of chalcogen precursors	Flow rates of N_2/H_2	Furnace temperature
WS_2	$(t\text{-BuN=})_2W(NMe_2)_2$, 50 sccm	$(t\text{-}C_4H_9)_2S_2$, 20 sccm	524/6 sccm	640 ºC
WSe_2	$(t\text{-BuN=})_2W(NMe_2)_2$, 50 sccm	$(C_2H_5)_2Se_2$, 20 sccm	524/6 sccm	640 ºC
MoS_2	$(t\text{-BuN=})_2Mo(NMe_2)_2$, 100 sccm	$(t\text{-}C_4H_9)_2S_2$, 50 sccm	444/6 sccm	590 ºC
$MoSe_2$	$(t\text{-BuN=})_2Mo(NMe_2)_2$, 50 sccm	$(C_2H_5)_2Se_2$, 50 sccm	494/6 sccm	640 ºC

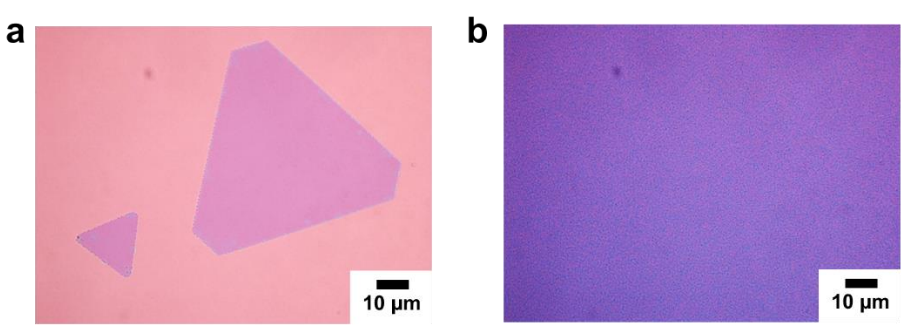

Figure S1. Optical microscopy images of WS_2 grown on SiO_2/Si via MOCVD (a) with and (b) without NaCl.

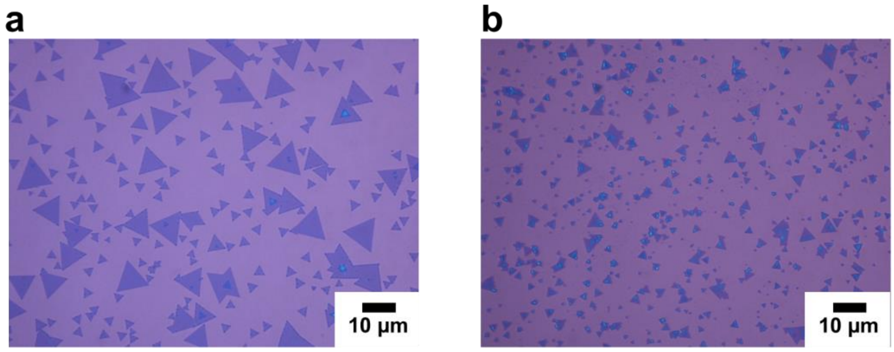

Figure S2. Optical microscopy images of $MoSe_2$ grown with different supply rates for the metal and chalcogen precursors. The N_2 bubbling rates through the Mo and Se precursors were (a) 50 and 50 sccm and (b) 50 and 200 sccm, respectively, and the combined N_2 and H_2 flow rate was 600 sccm.

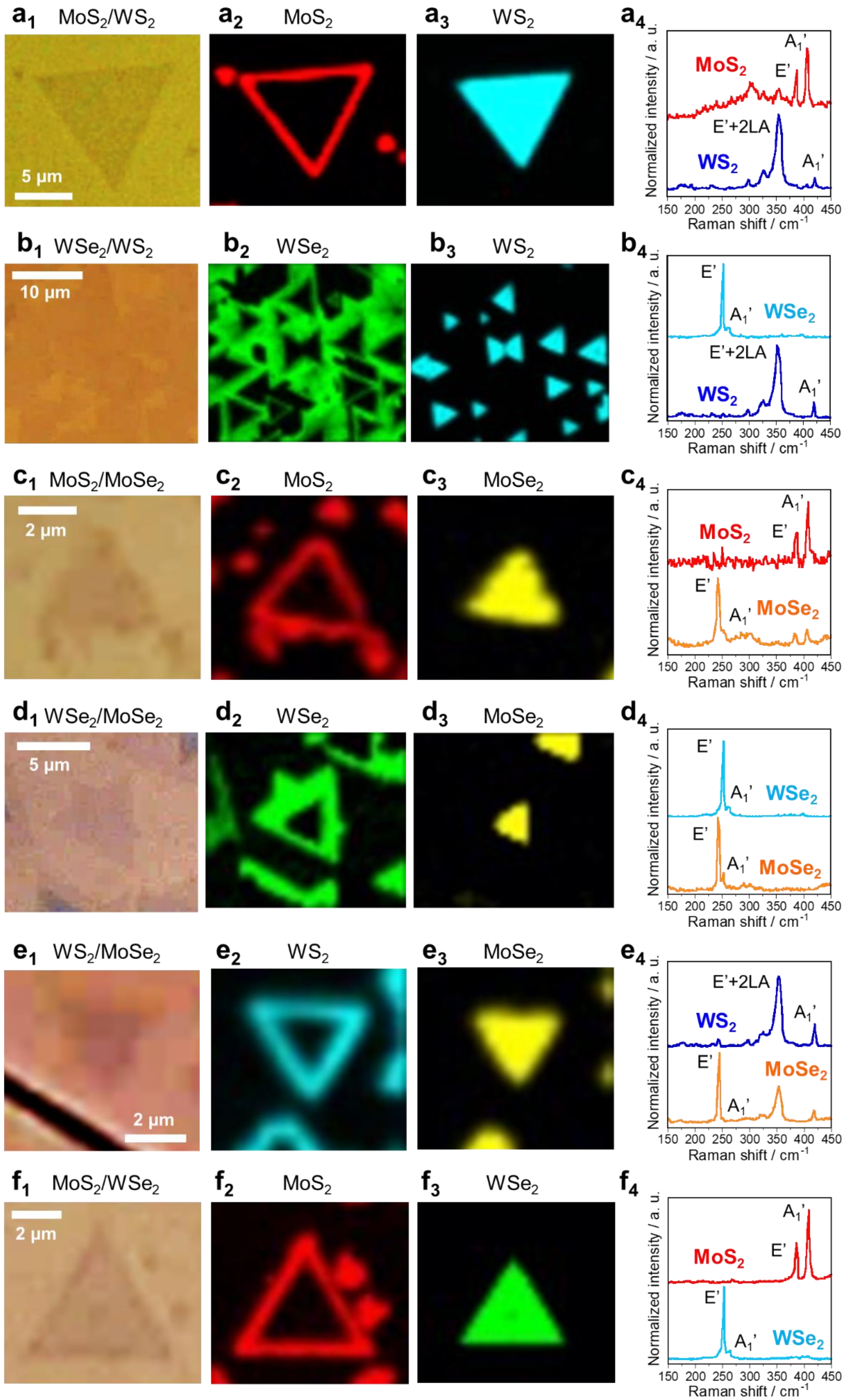

a1 MoS2/WS2
5 µm
a2 MoS2
a3 WS2
a4
MoS2
WS2
A1'
E'
E'+2LA
Normalized intensity / a. u.
Raman shift / cm-1
b1 WSe2/WS2
10 µm
b2 WSe2
b3 WS2
b4
WSe2
WS2
c1 MoS2/MoSe2
2 µm
c2 MoS2
c3 MoSe2
c4
MoSe2
d1 WSe2/MoSe2
5 µm
d2 WSe2
d3 MoSe2
d4
e1 WS2/MoSe2
2 µm
e2 WS2
e3 MoSe2
e4
f1 MoS2/WSe2
2 µm
f2 MoS2
f3 WSe2
f4
150 200 250 300 350 400 450

Figure S3. (a_1) Optical image, (a_2 and a_3) PL intensity maps (1.94 to 2.07 eV and 1.77 to 1.94 eV) and (a_4) Raman spectra of a MoS_2/WS_2 heterostructure. (b_1) Optical image, (b_2 and b_3) PL intensity maps (1.94 to 2.07 eV and 1.55 to 1.77 eV) and (b_4) Raman spectra of a WSe_2/WS_2 heterostructure. (c_1) Optical image, (c_2 and c_3) PL intensity maps (1.77 to 1.94 eV and 1.46 to 1.65 eV) and (c_4) Raman spectra of a $MoS_2/MoSe_2$ heterostructure. (d_1) Optical image, (d_2 and d_3) PL intensity maps (1.55 to 1.77 eV and 1.46 to 1.65 eV) and (d_4) Raman spectra of a $WSe_2/MoSe_2$ heterostructure. (e_1) Optical image, (e_2 and e_3) PL intensity maps (1.94 to 2.07 eV and 1.46 to 1.65 eV) and (e_4) Raman spectra of a $WS_2/MoSe_2$ heterostructure. (f_1) Optical image, (f_2 and f_3) PL intensity maps (1.77 to 1.94 eV and 1.55 to 1.77 eV) and (f_4) Raman spectra of a MoS_2/WSe_2 heterostructure. In the PL intensity maps, red, yellow, cyan and green correspond to the intensities of the MoS_2, $MoSe_2$, WS_2 and WSe_2 PL peaks, respectively.

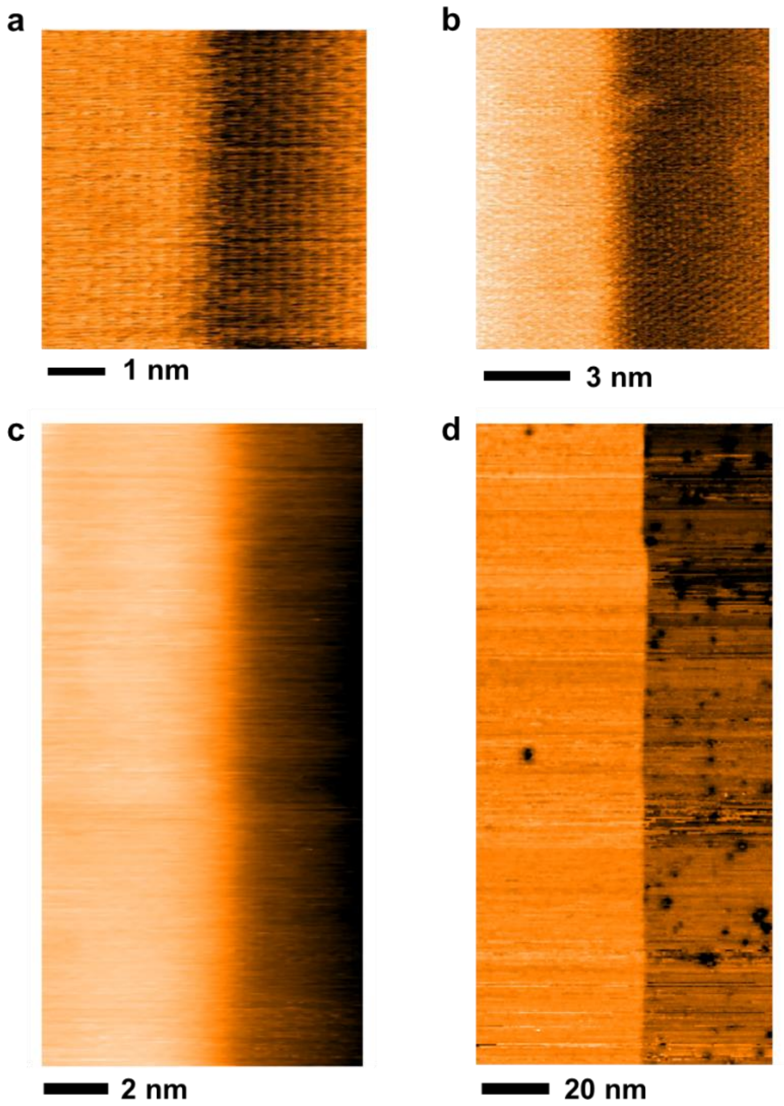

Figure S4 STM images of the MoS_2/WS_2 heterointerface from different regions. (V_s = + 1.2 V, (a) I_t = 0.2 nA, (b) 0.06 nA, and (c) 0.25 nA, (d) V_s = + 1.3 V, and I_t = 0.1 nA)

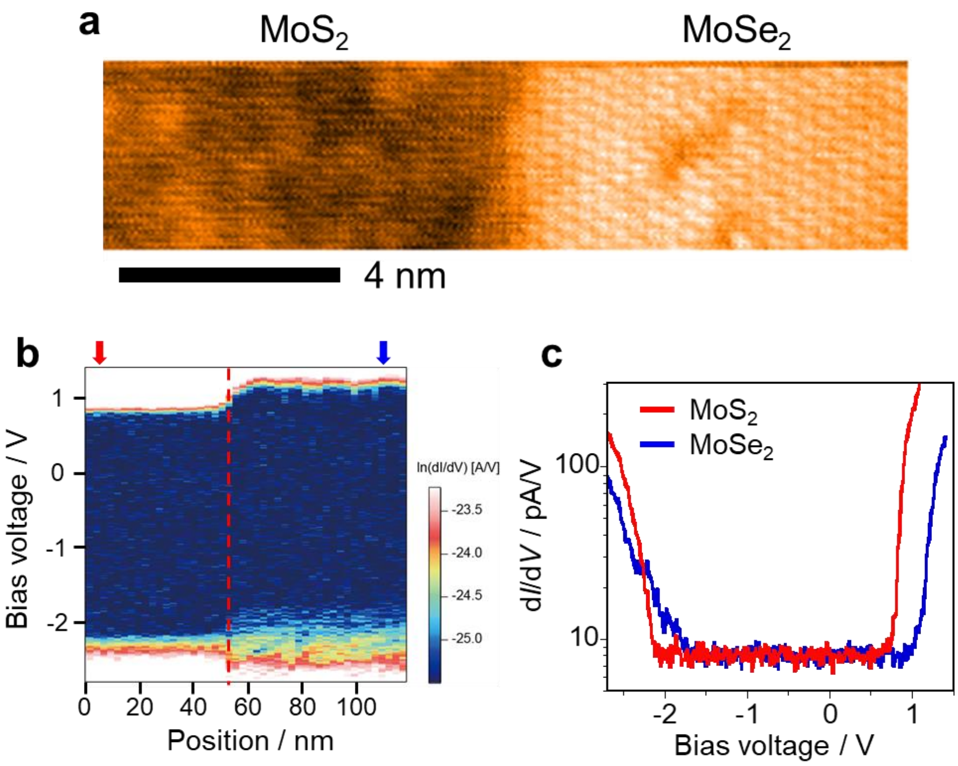

Figure S5. (a) STM image (V_s = + 2.2 V, I_t = 10 pA), (b) color scale map of the dI/dV spectra acquired in the vicinity of the heterointerface. (c) Averaged dI/dV spectra obtained from the MoS_2 and $MoSe_2$ regions. In (a), the presence of bright spots in MoS_2 (dark spots in $MoSe_2$) is derived from the changes of local density of state by chalcogen substitution.

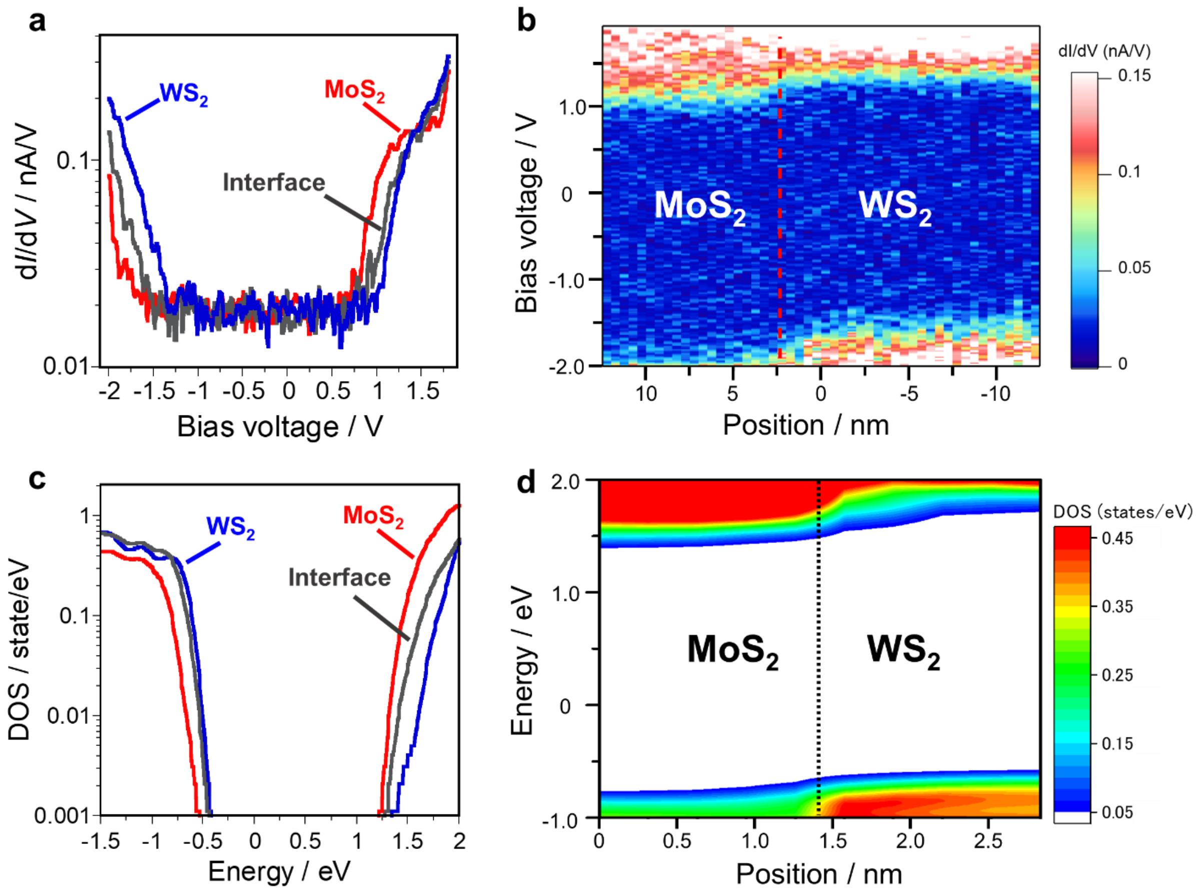

Figure S6. (a) Averaged dI/dV spectra obtained from the MoS_2, WS_2 and heterointerface regions. (b) Color scale map of the dI/dV spectra acquired in the vicinity of the heterointerface. (c) Calculated LDOS and (d) associated color scale map for the MoS_2/WS_2 heterostructure. In (b) and (d), the red and black dotted lines indicate the position of MoS_2/WS_2 heterointerface.

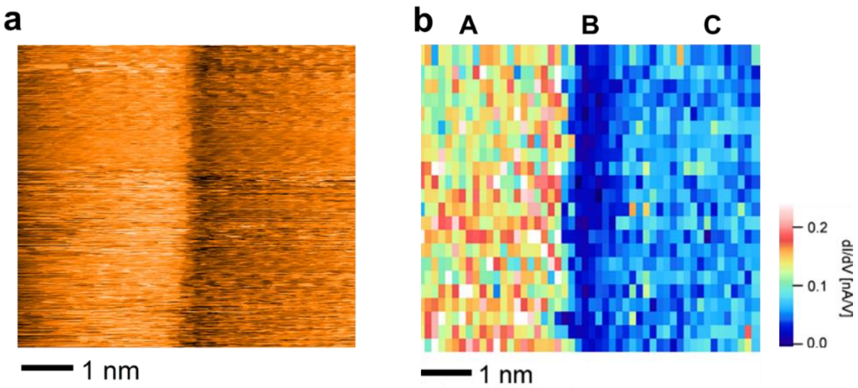

Figure S7. (a) STM image of the area around the MoS_2/WS_2 heterointerface (V_s = −2.5 V, I_t = 0.1 nA). (b) A dI/dV map acquired at a sample bias voltage of V_s = −2.19 V over the same area as in (a) (V_s = −2.5 V, I_t = 0.1 nA). It is noted that the inhomogeneous dots of the dI/dV signal are derived from measurement noise.

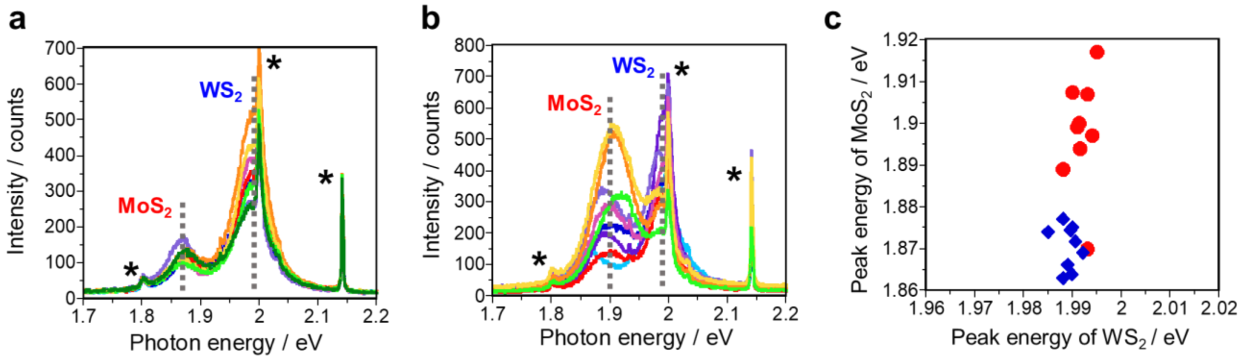

Figure S8. PL spectra of the WS_2/MoS_2 interfaces at different locations (a) within the identical grain and (b) in different triangle-shaped grains. Sharp peaks indicated by asterisks correspond to the Raman modes of the graphite substrate. (c) Plot of PL peak positions of MoS_2 and WS_2 at the interface within the same grain (blue diamonds) and in different triangle-shaped grains (red circles).

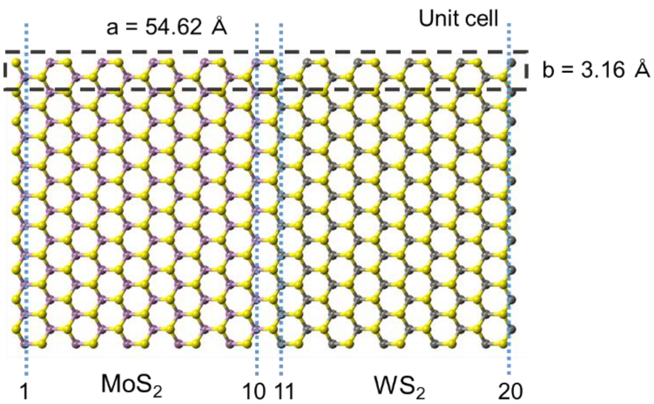

Figure S9. Unit cell of a superlattice consisting of WS_2 and MoS_2 strips with widths of 10 zigzag MoS_2 and WS_2 chains